Journal of Magnetism and Magnetic Materials 324 (2012) 3584–3587

Contents lists available at SciVerse ScienceDirect

Journal of Magnetism and Magnetic Materials

journal homepage: www.elsevier.com/locate/jmmm

Temperature and field dependent electronic structure and magnetic properties of $LaCoO_3$ and $GdCoO_3$

S.G. Ovchinnikov [a,b,*], Yu.S. Orlov [a], V.A. Dudnikov [a]

[a] Kirensky Institute of Physics, Siberian Branch, Russian Academy of Sciences, Akademgorodok, Krasnoyarsk 660036 Russia
[b] Siberian Federal University, Svobodnyi pr. 79, Krasnoyarsk 660041 Russia

ARTICLE INFO

Available online 3 March 2012

Keywords:
Electronic structure
Spin crossover
Insulator–metal transition

ABSTRACT

The transformation of the band structure of $LaCoO_3$ in the applied magnetic field has been theoretically studied. If the field is below its critical value $B_C \approx 65$ T, the dielectric band gap decreases with the field, thus giving rise to negative magnetoresistance that is highest at $T \approx 300 \div 500$ K. The critical field is related to the crossover between the low- and high-spin terms of Co^{3+} ions. The spin crossover results in an insulator–metal transition induced by an increase in the magnetic field. Similar calculations have been done for $GdCoO_3$ which is characterized by large spin gap ~ 2000 K.

1. Introduction

The perovskite-oxide $LaCoO_3$ has been studied intensely for many years due its unique magnetic properties and related insulator–metal transition (IMT) [1,2]. A gradual appearance of the paramagnetism above 50 K from the diamagnetic ground state in called the spin–state transition. Goodenough was the first who suggested that instead of the Hund's rule dictated high spin (HS) $S=0$ the strong crystalline electric field results in the low spin (LS) $S=0$ state for d^6 configuration of the Co^{3+} ion, and the energy difference is very small with the spin gap $\Delta_s = E(\mathrm{HS}) - E(\mathrm{LS}) \sim 100$ K. The thermal population of the HS state provides the sharp increase of the magnetic susceptibility χ with a maximum around 100 K. The large difference between the spin excitation gap Δ_S and the charge gap given by the activation energy for electrical conductivity $E_g \approx 0.1$ eV at low T indicates that $LaCoO_3$ is not a simple band insulator [3]. The second low peak in χ near $500 \div 600$ is often related to the insulator–metal transition (IMT). Surprisingly for the IMT electrical conductivity σ does not seem to show any noticeable anomaly at this temperature [3]. Moreover the discrepancy between the large charge gap $2E_a \approx 2300$ K and the $T_{IMT} \approx 600$ K implies that the IMT cannot be simply argued in terms of a narrow-gap semiconductor [4]. Here, we solved this problem by calculating the electronic band structure in the regime of strong electron correlations. We consider electron as the linear combination of quasiparticles (QP) given by excitations between the different multielectron configurations obtained by exact diagonalization of the CoO_6 cluster. With the Hubbard operators constructed within the exact cluster eigenstates we can calculate the QP band structure for the infinite lattice. The QP spectral weight is determined by the occupation numbers of the local multielectron configurations. We find that the thermal population of different sublevels of the $^5T_{2g}$ HS term split by the spin–orbital interaction results both in the spin state transition and also in some new QP excitations. Of particular importance is the hole creation QP from the initial d^6 HS into the d^5 HS term, this QP appears to form the in-gap state inside the large charge-transfer gap $E_g \approx 0.1$ eV. The intercluster hopping transforms this local QP into the in-gap band that lies just under the bottom of empty conductivity band and provides the insulating gap $2E_a \approx 0.2$ eV at $T=100$ K. It bandwidth increases with T, and overlapping with the conductivity band at $T=T^*=587$ K results in the IMT. Hence our approach allows treating both the low T spin–state transition and the high T_{IMT} on the same footing.

2. LDA+GTB calculations

Over the past 20 years the magnetic and electrical properties of cobaltates have been studied extensively both by theorists and experimentalists (see for a recent review [5]). The nature of the excited spin state above the singlet ^1A_g has been under debate. Besides the original $^5T_{2g}$ HS state with the $t_{2g}^4 e_g^2$ configurations there were many indications on the intermediate spin (IS) $S=1$ $^3T_{1g}$ state. The two stage model has been proposed with the LS–IS transition at 100 K and IS–HS transition at 550–600 K [6,7]. Recent electronic spin resonance (ESR) [8], the X-ray absorption spectroscopy (XAS) and X-ray magnetic circular dichroism

* Corresponding author at: Kirensky Institute of Physics, Siberian Branch, Russian Academy of Sciences, Akademgorodok, Krasnoyarsk 660036 Russia.
E-mail address: sgo@iph.krasn.ru (S.G. Ovchinnikov).

0304-8853/$ - see front matter © 2012 Elsevier B.V. All rights reserved.
doi:10.1016/j.jmmm.2012.02.096

(XMCD) [9] experiments prove that the lowest excited state is really the HS. Nevertheless the $^5T_{2g}$ term is splitted by the spin–orbital interaction in the low energy triplet with effective moment $J=1$, and higher energy sublevels with $J=2$ and $J=3$ [10].

$LaCoO_3$ as well as other strongly correlated oxides is a difficult problem for the ab initio band theory. The LDA calculations [11] incorrectly predict a metal for paramagnetic $LaCoO_3$. Various methods have been applied to study effect of correlations on the $LaCoO_3$ electronic structure: LDA+U or GGA+U [12–15], dynamical mean-field theory [16]. Recent variational cluster approximation (VCA) calculation [17] based on the exact diagonalization of the CoO_6 cluster gives a reasonably accurate description of the low temperature properties: the insulating nature of the material, the photoelectron spectra, the LS–HS spin–state transition. The main deficiency of the VCA is the failure to reproduce the high temperature anomalies in the magnetic and electronic properties associated with the IMT. To calculate the band dispersion in the strongly correlated material one has to go beyond the local multielectron configuration. The natural tool to solve this problem is given by the Hubbard X-operators $X_f^{pq}=|p\rangle\langle q|_{\vec{R}_f}$ constructed with the CoO_6 cluster eigenvectors $|p\rangle$ at site $\vec{R}_f$. All effects of the strong Coulomb interaction, spin–orbit coupling, covalency and the crystal field inside the CoO_6 cluster are included in the set of the local eigenstates E_p. Here p denotes the following quantum numbers: the number of electrons (both 3d Co and p of O), spin S and pseudoorbital moment $\tilde{l}$ (or the total pseudomoment $\tilde{J}$ due to spin–orbit coupling), the irreducible representation in the crystal field. A relevant number of electrons is determined from the electroneutrality, for stoichiometric $LaCoO_3$ $n=6$. In the pure ionic model the corresponding energy level scheme for d^6 Co^{3+} has been obtained in [10]. Due to the covalence there is admixture of the ligand hole configurations $d^{n+1}\underline{L}$ and $d^{n+2}\underline{L}^2$ that is very well known in the X-ray spectroscopy [18]. Contrary to spectroscopy the electronic structure calculations require the electron addition and removal excitations. For $LaCoO_3$ it means the d^5 and d^7 configurations. The total low energy eigenstates are shown in the Fig. 1. Here the energy level notations are the same as in the ionic model [10] but all eigenstate contains the oxygen hole admixture due to the covalence effect. The calculation of the $n=5$, 6, 7 eigenvectors for CoO_6 cluster with the spin–orbit coupling and the Coulomb interaction has been done in [19].

In the magnetic field the energy level scheme is given in the Fig. 2 where HS–LS crossover is seen at the critical field $V_C\approx 65$ T.

The electron removal spectrum determines the top of the valence band, the corresponding QP are shown in the Fig. 1 by thin solid lines as the excitation from the $^1A_1$ d^6 singlet in the $^2T_2$ d^5 states with $\tilde{J}=1/2$ and $\tilde{J}=3/2$. There energies are

$$\Omega_{V1}=E(d^6,{}^1A_1)-E(d^5,{}^2T_2,\tilde{J}=1/2)$$
$$\Omega_{V2}=E(d^6,{}^1A_1)-E(d^5,{}^2T_2,\tilde{J}=3/2) \quad (1)$$

The bottom of empty conductivity band has the energy

$$\Omega_C=E(d^7,{}^2E)-E(d^6,{}^1A_1) \quad (2)$$

All these bands have non-zero QP spectral weight determined by the occupation numbers of the initial and final states. The intercluster hopping results in the dispersion, $\Omega_n\to\Omega_n(k)$. The QP band structure corresponds to the charge-transfer insulator [20] with the gap $E_g\approx 1$ eV (Fig. 3) at $T=0$. This gap value is rather close to the VCA gap [17] and the experimental value $E_g\approx 1$ eV [4]. Spin crossover at B_C results in the IMT induced by magnetic field.

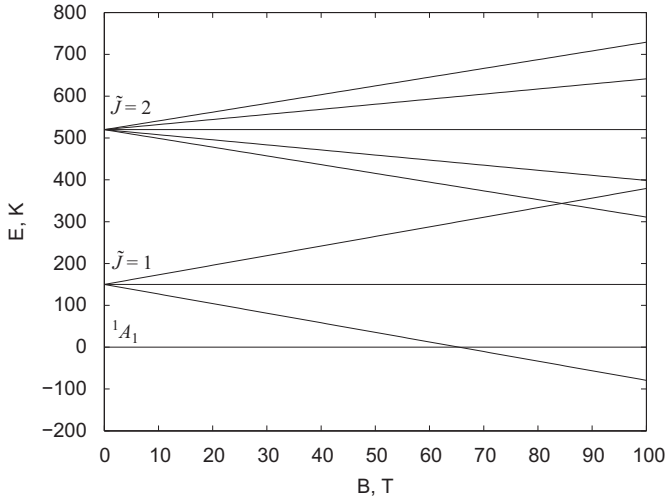

Fig. 2. Energies of the low-lying states of the Co^{3+} ion in the applied magnetic field.

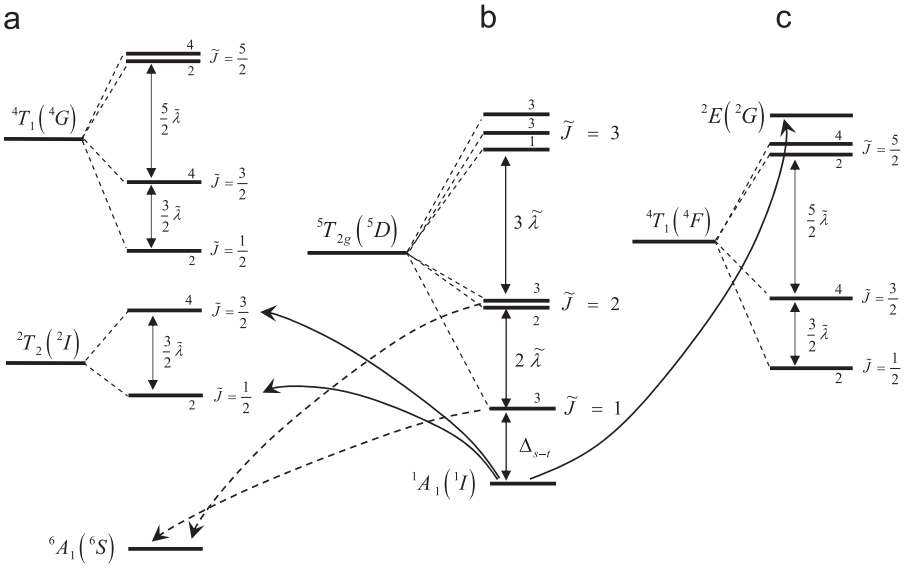

Fig. 1. Set of low-energy terms for (Ne=5, 6, and 7) electronic configurations in the crystal field. (a) N_e=5, (b) N_e=6, (c) N_e=7.

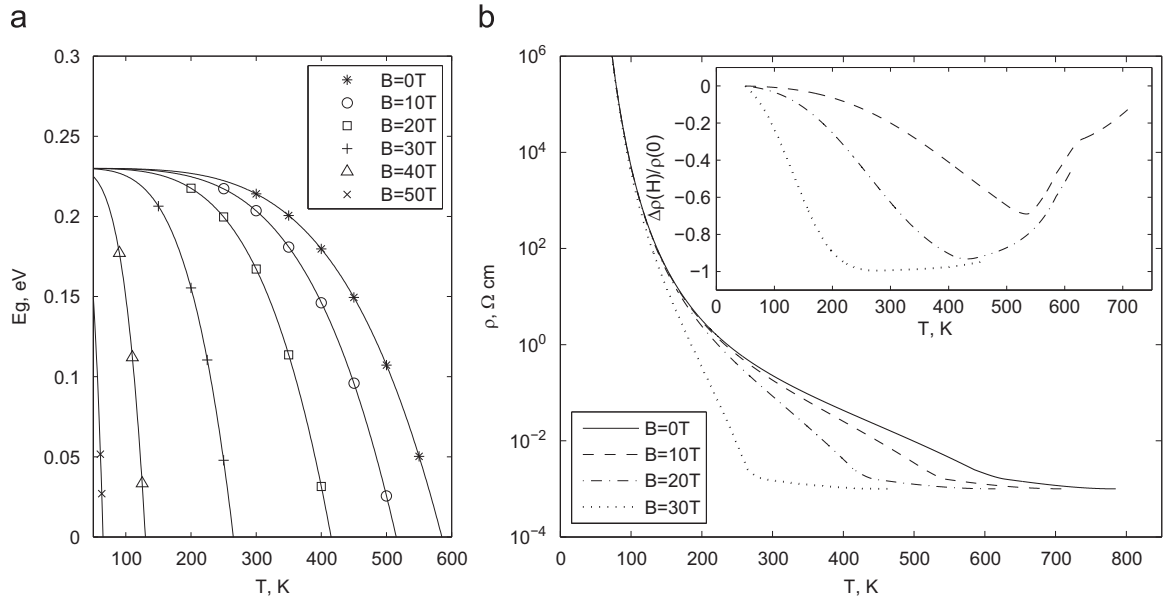

Fig. 3. Temperature dependences of the (a) dielectric band gap and (b) electrical resistance for various magnetic fields. The temperature dependence of the magnetoresistance $\Delta\rho/\rho=(\rho(B)-\rho(0))/\rho(0)$ at the same values of the applied magnetic field is shown in the inset.

At finite temperature the thermal excitation over the spin-gap Δ_{s-t} into the $\tilde{J}=1$ and over the gap $\Delta_{s-t}+2\tilde{\lambda}$ into the $\tilde{J}=2$ sublevels of the HS $^5T_{2g}$ state occurs. We take $\Delta_{s-t}=140$ K and $\tilde{\lambda}=-185$ K following [8]. Partial occupation of the excited HS states results in the drastically change of the QP spectrum. For $T=0$ excitations from the $^1A_1$ d^6 singlet in the lowest $^6A_1$ d^5 term were forbidden due to spin conservation, and the excitation from $d^6,\tilde{J}=1\rangle$ in $|d^5,^6A_1\rangle$ has non-zero matrix element (shown by dashed line Ω^*_{V1} in the Fig. 1) but zero filling factor as the excitation between two empty states. For $T\neq 0$ the filling factor for the Ω^*_{V1} and Ω^*_{V2} QP is non-zero and is equal to the occupation number n_1 and n_1 of the states $d^6,\tilde{J}=1\rangle$ and $d^6,\tilde{J}=2\rangle$ correspondingly. The energies of these QP are

$$\Omega^*_{V1}=E(d^6,^5T_{2g},\tilde{J}=1)-E(d^5,^6A_1)$$

$$\Omega^*_{V2}=E(d^6,^5T_{2g},\tilde{J}=2)-E(d^5,^6A_1) \quad (3)$$

The energies of these QP appear to be slightly below the bottom of the conductivity band, see DOS at finite temperature in the Fig. 4. Thus we have obtained that these temperature-induced QP states lies inside the charge-transfer gap, they are the in-gap states. The chemical potential lies in the narrow gap $2E_g\approx 0.2$ eV at $T=100$ K between the in-gap states and conductivity band.

From the GTB dispersion equation [21,22] it is clear that the in-gap bandwidth is proportional to the occupation numbers n_1 and n_2 of the excited HS states. With further temperature increase the in-gap bands Ω^*_{V1} and Ω^*_{V2} become wider and finally overlap with the conductivity band Ω_C at $T=T_*=587$ K. It should be clarified that the IMT in $LaCoO_3$ is not the thermodynamic phase transition, there is no any order parameter associated with the gap contrary to the classical IMT in VO_2, NiS etc.

We have also calculated the average moment $\vec{J}=\vec{L}+\vec{S}$ as $J_{av}=\langle J^2\rangle^{-1/2}$ as function of temperature (Fig. 4). Here

$$\langle J^2\rangle=\sum_n \langle n|J^2|n\rangle\langle X^{nn}\rangle \quad (4)$$

The expected for HS value $J_{av}\approx 2$ is reached only at $T\approx 1000$ K. In the region of the spin–state transition at $T\approx 100$ K the value of J_{av} is close to 1. May be it is the reason why so many experimentalists have obtained the IS $S=1$ fitting their data by the state with definite spin. Temperature dependence of the magnetic susceptibility has the maximum at $T\approx 100$ K similar to many previous works with LS–HS scenario [3,23].

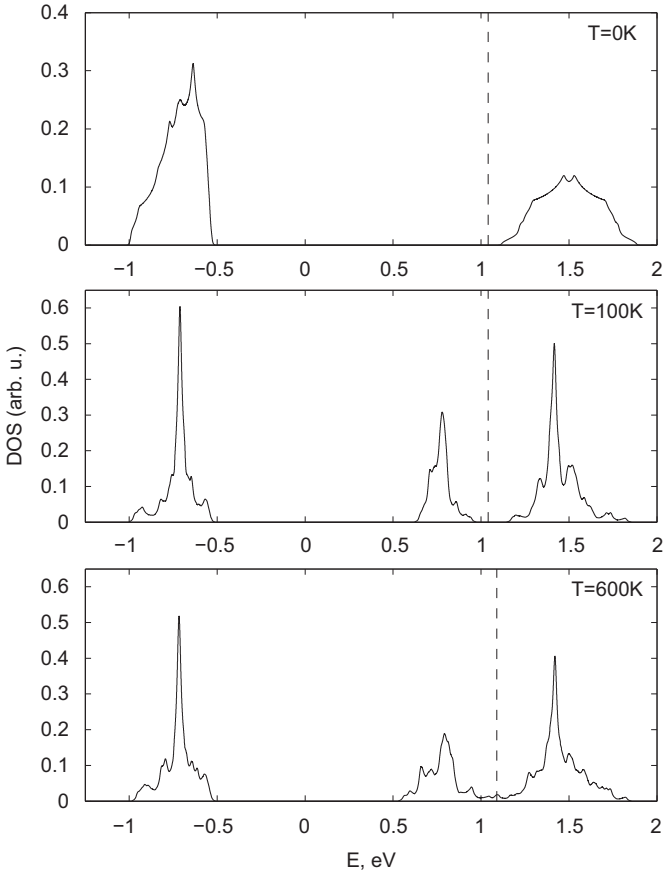

Fig. 4. Single particle density of states at different temperatures. At $T=0$ K $LaCoO_3$ is the insulator with the gap $E_g\approx 1.5$ eV. At finite temperatures the in-gap band appears below the conductivity band with the temperature dependent activation energy. At $T=100$ K $E_a\approx 0.1$ eV. At $T=T_{IMT}=587$ K $E_a=0$ eV, and above T_{IMT} the band structure is of the metal type.

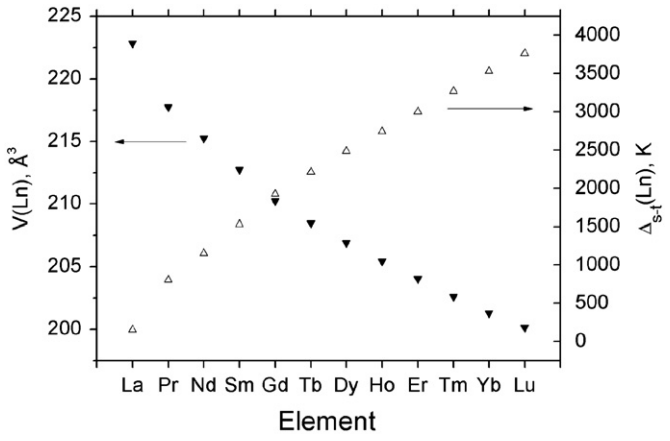

Fig. 5. Unit cell volume and the spin gap for all rare-earth elements.

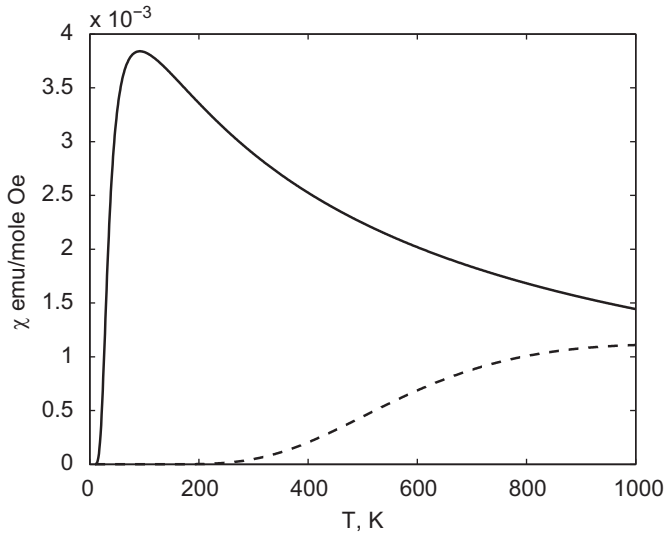

Fig. 6. Magnetic susceptibility of Co^{3+} ions in $LaCoO_3$ (solid line) and in $GdCoO_3$ (dashed line).

Substitution of La by a rare-earth element Ln results in a chemical pressure. Using the Berch–Murmagan equation of state we have estimated the value of chemical pressure and spin gap for all Ln elements (Fig. 5). For $GdCoO_3$ the spin gap is 2000 K. Magnetic susceptibility of Co^{3+} in $LaCoO_3$ and $LaCoO_3$ and $GdCoO_3$ are shown in Fig. 6. In $GdCoO_3$ there is also Cg^{3+} contribution [24].

3. Conclusion

Thus, we find that a correct definition of the electron in strongly correlated system directly results in the in-gap states during the spin–state transition due to the thermal population of the excited HS states. Close to the spin-state temperature region the in-gap states determine the value of the activation energy $E_a \approx 0.1$ eV. Further temperature increase results in large in-gap bandwidth and smaller E_a, and finally $E_a=0$ at $T^*=587$ K. As concerns the weak maximum in the $\chi(T)$ close to the IMT it may be a small Pauli-type contribution from the itinerant carriers above T^*. We emphasize that instead of rather large difference in temperatures of the spin–state transition ($\sim$100 K) and the IMT (600 K) the underlying mechanism is the same and is induced by the thermal population of the excited HS states. Large spin gap in $GdCoO_3$ shifts both $\chi(T)$ maximum and IMT to high temperatures above 1000 K.

Acknowledgments

We acknowledge discussions with G.A. Sawatzky, M.W. Haverkort, S.V. Nikolaev and V.A. Gavrichkov. This work is supported by the Siberia-Urals integration project no. 44, SBRAS project no. 38, Presidium RAS Program 20, RFBR Grant no. 10-02-00251.

References

[1] G.H. Jonker, J.H. Van Santen, Physica 19 (1953) 120–130.
[2] P.M. Raccah, J.B. Goodenough, Physical Review 155 (1967) 932–943.
[3] S. Yamaguchi, Y. Okimoto, H.H. Taniguchi, Y. Tokura, Physical Review 53 (1996) R2926.
[4] S. Yamaguchi, Y. Okimoto, Y. Tokura, Physical Review B 54 (1966) R11022.
[5] N.B. Ivanova, S.G. Ovchinnikov, M.M. Korshunov, I.M. Eremin, N.V. Kazak, Uspekhi Fizicheskikh Nauk 179 (2009) 837–860;
N.B. Ivanova, S.G. Ovchinnikov, M.M. Korshunov, I.M. Eremin, N.V. Kazak, Physics-Uspekhi 52 (2009) 789–810.
[6] R.H. Potze, G.A. Sawatzky, M. Abbate, Physical Review B 51 (1995) 11501–11506.
[7] T. Saitoh, T. Mizokawa, A. Fujimori, M. Abbate, Y. Takeda, M. Takano, Physical Review B 55 (1997) 4257–4266.
[8] S. Noguchi, S. Kawamata, K. Okuda, H. Najiri, M. Motokawa, Physical Review B 66 (2002) 094404.
[9] M.W. Haverkort, Z. Hu, J.C. Cezar, T. Burnus, H. Hartmann, M. Reuther, C. Zobel, T. Lorenz, A. Tanaka, N.B. Brookes, H.H. Hsieh, H.-J. Lin, C.T. Chen, L.H. Tjeng, Physical Review Letters 97 (2006) 176405.
[10] Z. Ropka, R.J. Radwanski, Physical Review B 67 (2003) 172401.
[11] P. Ravindran, P.A. Korzhavye, H. Fjellvag, A. Kjekshus, Physical Review B 60 (1999) 16423–16434.
[12] M.A. Korotin, S.Yu. Ezhov, I.V. Solovyev, V.I. Anisimov, Physical Review B 54 (1966) 5309.
[13] K. Knizek, P. Novak, Z. Jirak, Physical Review B 71 (2005) 054420.
[14] S.K. Randey, Ashwani Kumar, S. Patil, V.R.R. Medicherla, R.S. Singh, K. Maiti, D. Prabhakaran, A.T. Boothroyd, A.V. Pimpale, Physical Review B 77 (2008) 045123.
[15] H. Hsu, K. Umemoto, M. Coccoccioni, R. Wentzcovitch, Physical Review B 79 (2009) 125124.
[16] L. Craco, E. Muller-Hartmann, Physical Review B 77 (2008) 045130.
[17] R. Eder, Physical Review B 81 (2010) 035101.
[18] M. Abbate, J.C. Fuggle, A. Fujimori, L.H. Tjeng, C.T. Chen, R. Potze, G.A. Sawatzky, H. Eisaki, S. Uchida, Physical Review B 47 (1993) 16124.
[19] Yu.S. Orlov, S.G. Ovchinnikov, Journal of Experimental and Theoretical Physics 109 (2009) 322–338.
[20] J. Zaanen, G.A. Sawatzky, J.W. Allen, Physical Review Letters 55 (1985) 418.
[21] V.A. Gavrichkov, A.A. Borisov, S.G. Ovchinnikov., Physical Review B 64 (2001) 235.
[22] M.M. Korshunov, V.A. Gavrichkov, S.G. Ovchinnikov, Z.V. Pchelkina, I.A. Nekrasov, M.A. Korotin, V.I. Anisimov, Journal of Experimental and Theoretical Physics 99 (2004) 559.
[23] M.J.R. Hoch, S. Nellutla, J. van Tol, Eun Sang Choi, Jun Lu, H. Zheng, J.F. Mitchell, Physical Review B 79 (2009) 214421.
[24] V.A. Dudnikov, S.G. Ovchinnikov, Yu.S. Orlov, N.V. Kazak, C.M. Michel, S.G. Patrin, G.Yu. Yur'ev, JETP, submitted for publication.